

# Ferromagnetism in Nitrogen-doped MgO

Phivos Mavropoulos,\* Marjana Ležaić,<sup>†</sup> and Stefan Blügel  
*Institut für Festkörperforschung (IFF) and Institute for Advanced Simulation (IAS),  
 Forschungszentrum Jülich, D-52425 Jülich, Germany*

The magnetic state of Nitrogen-doped MgO, with N substituting O at concentrations between 1% and the concentrated limit, is calculated with density-functional methods. The N atoms are found to be magnetic with a moment of  $1 \mu_B$  per Nitrogen atom and to interact ferromagnetically via the double exchange mechanism. The long-range magnetic order is established above a finite concentration of about 1.5% when the percolation threshold is reached. The Curie temperature  $T_C$  increases linearly with the concentration, and is found to be about 30 K for 10% concentration. Besides the substitution of single Nitrogen atoms, also interstitial Nitrogen atoms, clusters of Nitrogen atoms and their structural relaxation on the magnetism are discussed. Possible scenarios of engineering a higher Curie temperature are analyzed, with the conclusion that an increase of  $T_C$  is difficult to achieve, requiring a particular attention to the choice of chemistry.

PACS numbers: 75.50.Pp, 75.50.Hx, 75.30.Et

## I. INTRODUCTION

In the research field of diluted magnetic semiconductors (DMS), a new direction is being investigated in the last five years, namely the engineering of ferromagnetic state formation by *sp* impurity doping. Compared to the more traditional DMS with transition-metal impurities, the novel *sp*-magnetism, or *d<sup>0</sup>*-magnetism, is rather unexplored. The increasing interest is due to the perhaps unexpected finding that *p*-bands can spontaneously polarize giving a ferromagnetic state (although the possibility of magnetic *sp*-defects is long known), but also due to the hope of tuning the properties of these states so that high Curie temperatures are achieved even at low concentrations.

Theoretical considerations have revealed mainly two routes for the formation of *sp*-ferromagnetic states. In the first, the semiconductor or insulator cation is substituted by an atom of smaller valency, thus depriving the *p*-type valence band from electrons. This hole-doping can shift the Fermi level into the valence band deep enough that the Stoner criterion is fulfilled, and spontaneous spin polarization appears (see Fig. 1a). This is, for example, the mechanism encountered in alkali-atom doped TiO<sub>2</sub> and ZrO<sub>2</sub>, predicted to be ferromagnetic by *ab-initio* calculations.<sup>1</sup> The hole-doping can also be achieved by cation vacancies, instead of substitution, as was e.g. proposed for the cases of HfO<sub>2</sub>, CaO, and ZrO<sub>2</sub>.<sup>2,3,4</sup>

The second scenario is that the anion is substituted by one of smaller valency, introducing shallow, spin-polarized gap states. As the impurity concentration increases, these states form impurity bands, which remain spin-polarized if the Stoner criterion is fulfilled (see Fig. 1b). The magnetic moment is expected to be strongest for *2p* impurities, i.e., in the case in Carbon- or Nitrogen-doped oxides.<sup>5,6,7,8,9,10,11,12,13</sup> This is because the *2p* states have no nodes and are rather localized, leading to a significant Hund's-type exchange interaction on-site. In the concentrated limit (full substitution of the anion, see e.g. Ref. 14), both routes converge to the same

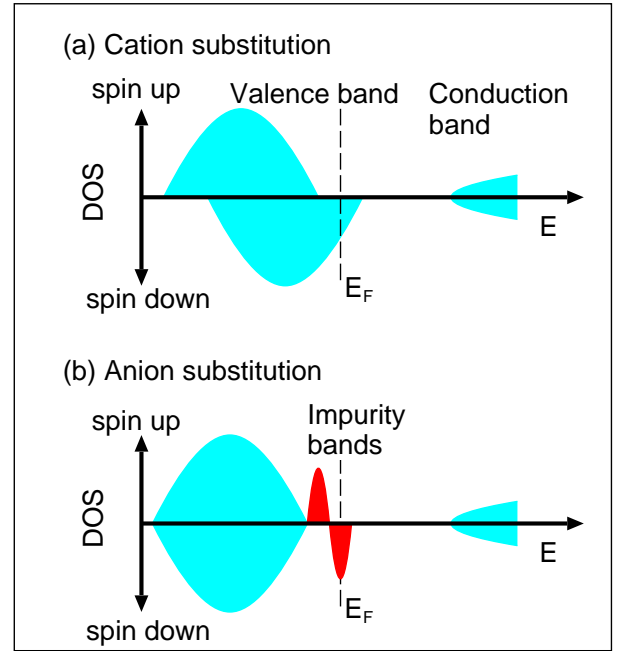


FIG. 1: (color online) Typical mechanisms for *sp* ferromagnetism: (a) cation substitution drives the Fermi level  $E_F$  into the valence band; (b) anion substitution creates an impurity band in the gap.

mechanism.

While the appearance of *p*-type magnetic states in oxides has been studied in the past, preliminary predictions of the Curie temperature have been so far based only on mean-field theory,<sup>5,6,11</sup> which has since been shown to give qualitatively wrong results, overestimating  $T_C$ , because it ignores the fundamental phenomenon of magnetic percolation in diluted disordered magnetic systems.<sup>15,16,17</sup> This means that, at low concentrations, the average inter-impurity distance is large, so that the short-range exchange interactions cannot produce a high

Curie temperature although they are strong.

The scope of this paper is to investigate the appearance and stability of the ferromagnetic state, including calculations for the Curie temperature, in  $\text{MgO}_{1-x}\text{N}_x$  compounds for  $x < 15\%$ , in view of recent experimental activities in the particular system.<sup>18</sup> Our focus is on the solution provided by local density-functional theory (DFT), presented in Sec. II, and on the calculation of the Curie temperature (Sec. III) with the exchange constants harvested within the adiabatic approximation. As it turns out, for any reasonable concentration the Curie temperatures are significantly lower than room temperature, therefore, we also explore the possibility of increasing the Curie temperature by heavy doping in Sec. IV. Further on, we discuss the physics that lies beyond our approximations in Sec. V. There, among our considerations, a comparison is made to previously calculated results for N-doped MgO that focus on the effects of electron correlation, and we also explore the constraints imposed by our specific structural model, including a discussion on the solubility of N in MgO. Finally, we give an outlook in Sec. VI. The methods of calculation are shortly described in the Appendix.

## II. GROUND-STATE ELECTRONIC AND MAGNETIC STRUCTURE

MgO crystallizes in the rock-salt structure with a lattice parameter of 4.21 Å and exhibits a wide band gap of 7.8 eV. In our density-functional calculations the gap is found to be 4.8 eV, due to the well-known underestimation of insulator band gaps within local density-functional theory [local density approximation (LDA) or generalized gradient approximation (GGA)]. When substituting O, N induces  $p$  states in the MgO gap, approximately 0.5 eV above the valence band edge. As N has one electron less than O, the gap states host one unpaired hole, showing a magnetic moment of  $1 \mu_B$  per N atom.

At finite concentrations, interaction among the impurity states forms a partially filled impurity band. The spin polarization remains present even at high concentrations, showing that magnetism is not only a consequence of the missing electron, but also of the relatively strong Hund's exchange due to the localization of the  $2p$  states. The spin-polarized density of states shows a half-metallic behavior, as we found by calculations with the Korringa-Kohn-Rostoker Green function method<sup>31</sup> (KKR) within the Coherent Potential Approximation to disorder (CPA). (Details on the calculation methods are given in the Appendix.) Through a calculation of structural relaxation around a N impurity, performed with the VASP<sup>19</sup> projector augmented wave code at 5% concentration in supercell geometry, we could rule out serious Jahn-Teller distortions around the impurity: the first neighbors relax outward by less than 2%, including only a weak symmetry breaking along one of the three crystallographic axes. This leads to a small lifting of degeneracy

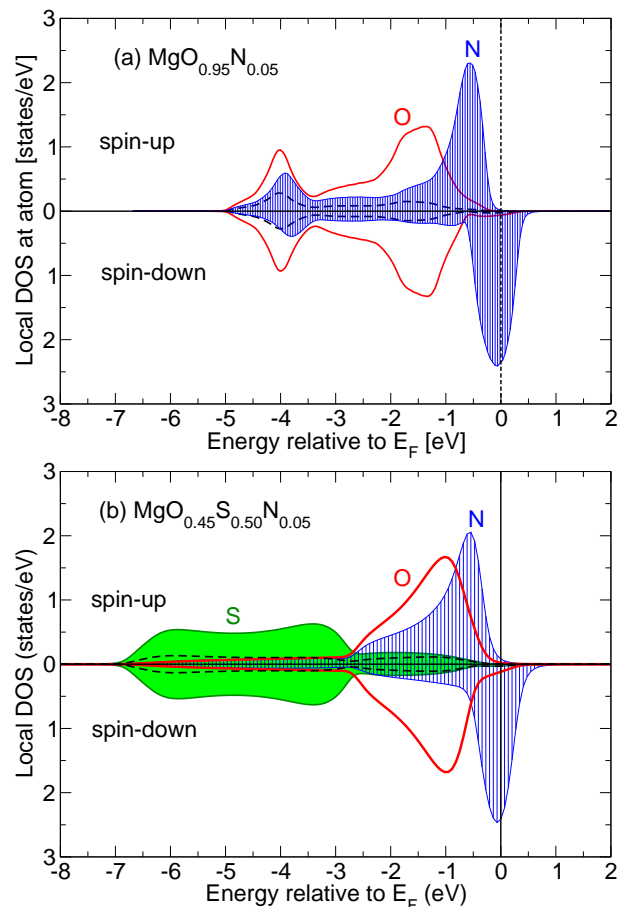


FIG. 2: (color online) (a) Atom-resolved local densities of states (LDOS) of  $\text{MgO}_{0.95}\text{N}_{0.05}$  calculated within the KKR-CPA. The LDOS of the Mg atom is presented by a dashed line. (b) Same for  $\text{MgO}_{0.45}\text{S}_{0.50}\text{N}_{0.05}$ .

of the impurity state, insignificant compared to the impurity band width. The small atomic displacements also justify the use of CPA.

We turn now to the discussion of the electronic and magnetic structure. Fig. 2(a) shows the atom-resolved local densities of states (DOS) at a N concentration of  $x=5\%$ . Evidently N has a spin-split DOS and exhibits a local magnetic moment. The N majority-spin (spin-up) impurity band is fully occupied and the minority-spin (spin-down) impurity band is occupied by 2/3. As a consequence, 1/3 the total moment is  $1 \mu_B$  per N atom. At lower concentrations the DOS is very similar, but with smaller impurity band width  $w$  ( $w$  depends on the concentration as  $w \sim \sqrt{x}$ , since  $x$  represents an average number of impurity neighbors, and it is known from the tight-binding approximation that  $w$  increases as the square root of the number of neighbors). The exchange splitting is of the order of 0.5 eV, giving an exchange integral of  $I = 0.5 \text{ eV}/\mu_B$ , which is approximately half the one in 3d transition metals.

Already from examining the ferromagnetic density

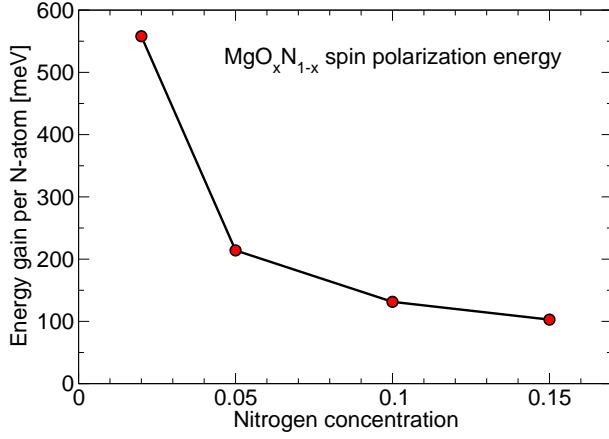


FIG. 3: Spin-polarization energy per Nitrogen atom as a function of concentration  $x$ . As the concentration increases, the hybridization increases, the impurity band becomes more itinerant, and the spin-polarization energy per atom drops. The line is a guide to the eye.

of states it is expected that the ferromagnetic state will be stable, since  $E_F$  lies within the impurity band, favoring double-exchange<sup>20,21</sup> (i.e., upon ferromagnetic alignment, hybridization leads to a broadening of the partially-filled impurity-band, resulting in energy gain). We confirmed this by calculations (not shown here in detail) of the total energy of the ferromagnetic state,  $E_{\text{ferro}}$ , versus the disordered-local-moment state energy,  $E_{\text{DLM}}$ ; the latter is represented in the CPA by an alloy of the type  $\text{MgO}_{1-x}\text{N}_{0.5x}^{\uparrow}\text{N}_{0.5x}^{\downarrow}$ , where  $\text{N}^{\uparrow}$  and  $\text{N}^{\downarrow}$  are impurities with magnetic moment pointing “up” and “down”.<sup>20</sup> As is typical for double-exchange DMS systems,<sup>15</sup> we found that the energy gain of the ferromagnetic state,  $E_{\text{DLM}} - E_{\text{ferro}}$ , scales with the square root of the concentration. Further confirmation on the ferromagnetic nature of the ground state comes from calculations of the exchange constants, to be presented in the next Section.

The spin polarization energy (i.e., the energy gain of the system due to the moments’ formation) drops with concentration due to the increase of hybridization, ranging between 550 and 100 meV for  $2\% < x < 15\%$ , as can be seen in Fig. 3. However, a high spin-polarization energy is a necessary but not sufficient condition for the stability of the ferromagnetic state and for a high Curie temperature. The extension of the impurity gap-state is also important, as it dictates the “communication” between localized moments and determines the onset of magnetic percolation.<sup>15,16</sup> We therefore show in Fig. 4(a) the extension of the Nitrogen-induced spin-polarized hole (calculations here were done within the KKR impurity-in-host approach, assuming that the three N-induced gap states are degenerate and occupied by 2/3 each). We find that approximately half of the hole is localized at the impurity site, while most of the remaining charge is distributed at the 12 nearest Oxygen neighbors. From Fig. 4(b) it can also be seen that the hole falls off ex-

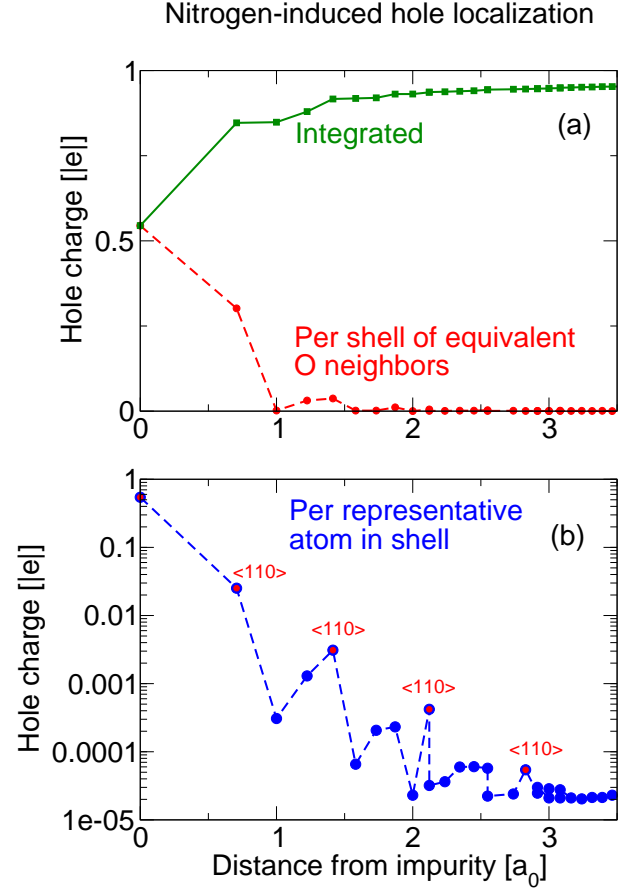


FIG. 4: (color online) Spatial distribution of the Nitrogen-induced spin-polarized hole for the case of a single Nitrogen impurity substituting O in MgO. Only the fraction of the hole at the N and O atoms is presented (the fraction at the Mg atoms is negligible). The distribution of the magnetic moment ( $1 \mu_B$ ) is practically the same. (a) Full (green) curve: Integrated hole charge as a function of distance from the impurity. Dashed (red) curve: Hole charge per shell of O atoms that are equidistant from N and equivalent by the point-group symmetry. The impurity accommodates more than half of the hole charge. (b) Hole charge per atom as a function of distance from the impurity. Only one of the symmetry-equivalent atoms is considered for every shell. The points labelled  $\langle 110 \rangle$  represent atoms in the  $\langle 110 \rangle$  direction, in which the extent of the impurity wavefunction is largest.  $a_0$  is the lattice parameter.

ponentially with distance, showing, however, a higher value in the  $\langle 110 \rangle$  directions. These are the directions of the first Oxygen neighbors in the fcc lattice (which is the sublattice formed by Oxygen atoms in MgO), and in these directions also the pair exchange constants fall off slower (see Sec. III). The hole occupation at Mg sites is negligible.

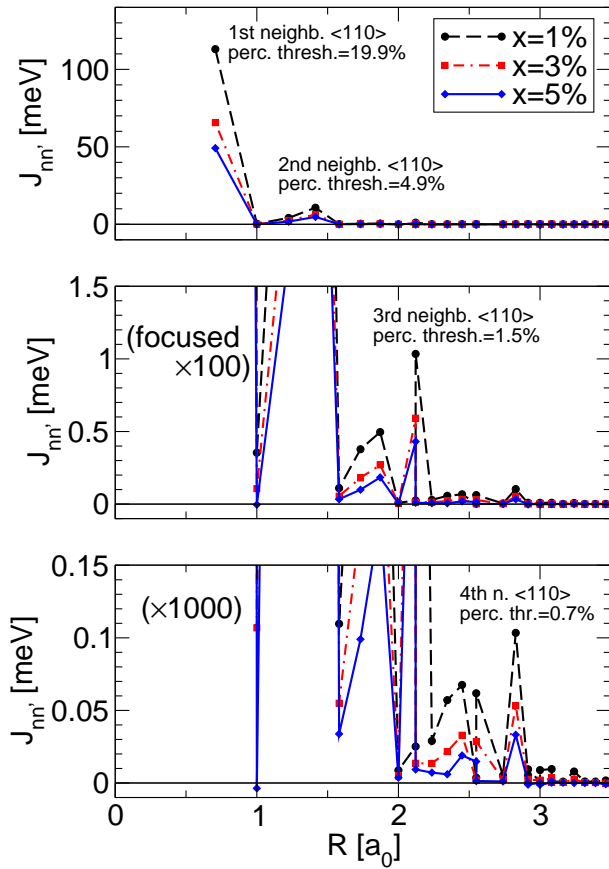


FIG. 5: (color online) Pair exchange interactions  $J_{nn'}$  as a function of distance  $R$  between nitrogen atoms for  $x = 1\%$ ,  $3\%$ , and  $5\%$ . The peaks corresponding to neighbors in the  $\langle 110 \rangle$  directions are indicated, together with the percolation threshold for interactions up to the particular distance.  $a_0$  is the lattice parameter. The lines are guides to the eye.

### III. EXCHANGE INTERACTIONS AND CURIE TEMPERATURE

We turn now to the discussion of the Curie temperature. We describe the fluctuations of the magnetization on the basis of the classical Heisenberg Hamiltonian,  $H = -\sum_{nn'} J_{nn'} \hat{e}_n \cdot \hat{e}_{n'}$ . Here,  $J_{nn'}$  are the pair exchange parameters between N impurities at sites  $n$ ,  $n'$  and  $\hat{e}_n$ ,  $\hat{e}_{n'}$  are unit vectors pointing in the direction of the local moments. The Heisenberg model includes the transversal degrees of freedom of the fluctuating magnetic moments. As we see below, this energy scale is much smaller than the spin-polarization energy, and thus the longitudinal fluctuations of the magnetic moments are safely ignored as regards the Curie point.

The  $J_{nn'}$  are fitted to LDA results so that at the end the magnetic excitation energies of the Heisenberg Hamiltonian correspond to the ones of  $\text{MgO}_{1-x}\text{N}_x$ . For the fitting we employ the method of infinitesimal rotations.<sup>22</sup> The results are shown in Fig. 5. Clearly, all interactions are ferromagnetic. We note that there is a marked con-

centration dependence, with stronger exchange constants at low concentrations, as is well-known in DMS systems with double-exchange ferromagnetic interactions (see, for example, Ref. 23).

Note, however, that there is a “hidden” antiferromagnetic superexchange interaction, reducing the value of  $J_{nn'}$ . This arises from the proximity of the impurity bands of both spins to  $E_F$ : in an antiferromagnetic alignment of two impurities, energy is gained due to hybridization of majority-spin states of each impurity with minority-spin states of the other, accompanied by downward shifting of the occupied majority-spin bands and upward shifting of the minority-spin bands.<sup>23</sup> This superexchange counter-acts the double exchange to some extent. To reveal this, we performed a non-self-consistent calculation of  $J_{nn'}$  (just one iteration) after shifting the majority-spin potential of N to lower energies by 2.7 eV. In this way the majority-spin N band is driven away from the Fermi energy and superexchange is strongly reduced. The result (not shown here) was striking: the  $J_{nn'}$  became stronger by approximately 50% even at long distances.

It is evident that the nearest-neighbor exchange constants are large (Fig. 5), though insignificant, in the dilute case, for the stability of the ferromagnetic state; this is governed by longer-range exchange, due to the requirement for magnetic percolation.<sup>15,16</sup> However, the  $J_{nn'}$  fall off exponentially with distance, as is expected by the fact that the Fermi level falls in the gap at least for the one spin direction<sup>24</sup> (half-metallic or insulating systems). Notably, the slowest decay of  $J_{nn'}$  is observed along  $\langle 110 \rangle$ , i.e., in the directions where the charge of the impurity gap-state falls off with the slowest rate (see also Fig. 4). Note that the interactions in the  $\langle 110 \rangle$  directions are also dominating in zinc-blende or diamond-structure DMS with transition-element impurities.<sup>25,26</sup>

In Fig. 5 we also give the percolation thresholds which we calculated for interaction distances corresponding to “peaks” of  $J_{nn'}$  in the  $\langle 110 \rangle$  directions. We see that the nearest-neighbor coupling starts playing a role at  $x = 20\%$ , while the next peak, corresponding to  $R = \sqrt{2}a_0$ , becomes important only for concentrations above  $x = 4.9\%$ ; at this concentration,  $J(\sqrt{2}a_0) \approx 5$  meV. At concentrations of the order of 1.5%, where we see the onset of the Curie temperature in Fig. 6 (discussed in more detail below), the third neighbor in the  $\langle 110 \rangle$  direction becomes important, with a low value of  $J(\frac{\sqrt{3}}{2}a_0) \approx 1$  meV. We consider interactions beyond this distance as negligibly small, therefore we recognize the concentration of 1.5% as a magnetic percolation threshold for  $\text{MgO}_{1-x}\text{N}_x$ ; this can be seen also from the concentration-dependent Curie temperature, as we discuss below. (Of course  $J(R)$  is never *exactly* zero, therefore the choice of  $x = 1.5\%$  as percolation threshold is somewhat arbitrary, but, we think, reasonable.)

A strong exponential decrease of  $J_{nn'}$  is an indication of a low Curie temperature in diluted magnetic systems. We have calculated  $T_C$  within the random-phase



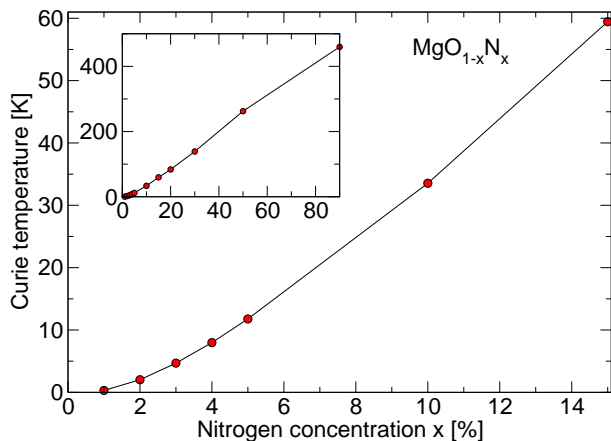


FIG. 6: Curie temperatures for N concentrations between 1% and 15%, calculated within the RPA. Inset: Same in the concentration range below 1-90%. The lines are guides to the eye.

approximation for disordered systems, following the prescription of Hilbert and Nolting<sup>17</sup> (see the Appendix for calculational details). In doing this, we assumed the limit of classical spins ( $S \rightarrow \infty$ , with appropriate renormalization of the exchange constants), for reasons that we discuss in Sec. V. In special cases we also performed Monte Carlo calculations, as described in the Appendix, which gave typically 50% higher  $T_C$ . The results on the Curie temperature, as a function of concentration, are shown in Fig. 6. Although in this work we are interested in concentrations up to the order of  $x = 10$ -15%, in the calculation we included also high concentrations, in order to see the trend when approaching the concentrated limit. Starting from a percolation threshold at approximately  $x = 1.5\%$ ,  $T_C$  rises linearly with concentration. Although, as we saw, the exchange constants at any particular distance weaken with increasing concentration, the important effect here comes from the decrease of the average inter-impurity distance at higher  $x$ , allowing for the shorter-ranged, stronger interactions to play a role in the ferromagnetic ordering.

At concentrations that are usually considered in DMS systems, i.e., not higher than 10-15%, the Curie temperature turns out to be rather low: we find  $T_C = 35$  K at 10%, and even at  $x = 20\%$ ,  $T_C$  is still below 100 K. This is a clear drawback for application purposes at room temperature, and in the following Section we consider possible ways to overcome this difficulty.

#### IV. CONSIDERATIONS ON HOW TO INCREASE $T_C$

Since the Curie temperature of diluted magnetic systems depends on the long-range exchange constants, we have examined several possibilities of increasing  $J_{nn'}$  at distances larger than nearest neighbors. Considering

that  $J_{nn'}$  falls off exponentially with distance  $R_{nn'} = |\vec{R}_n - \vec{R}_{n'}|$  with a characteristic decay parameter  $\kappa$ ,  $J_{nn'} \sim \exp(-\kappa R_{nn'})$ , the main scope is to reduce  $\kappa$ . We tried to do this in several ways, as we discuss here, however, none produced a significant improvement.

–*Reducing the band gap.* Perhaps the most obvious way to reduce  $\kappa$  is to engineer a smaller gap by alloying. For instance,  $\text{Mg}_{1-x}\text{Zn}_x\text{O}$  shows a smaller gap, while retaining the rock-salt structure at not too high Zn concentrations; numerous other alloying combinations could have a similar effect. We pursued this idea by acting with an attractive constant potential on the Mg site, thus artificially reducing the MgO gap size. We then derived  $\kappa(E)$  by calculating the complex band structure for energies in the gap region, i.e., looking for solutions of the Schrödinger equation that fall off as  $\psi \sim e^{-\kappa r}$  (this procedure is well-known in the calculation of surface and interface states). For  $E$  deep in the gap there is a significant reduction of  $\kappa(E)$  with the gap size. However, for  $E$  at the actual position of the N levels (relatively close to the valence band edge  $E_v$ ),  $\kappa(E)$  is mainly determined by the effective mass  $m^*$  of the light-hole valence band as  $\kappa \approx \sqrt{2m^*(E - E_v)}/\hbar$ , due to the analytical behavior of the complex band structure. (Note that, among the complex bands, we seek the one with smallest value of  $\kappa$ , which corresponds to the band derived from the light holes.<sup>27</sup>) As the effective mass does not change appreciably, we find that a reduction of the gap does not affect  $\kappa(E_F)$  significantly, thus it cannot change the long-range exchange coupling.

–*Changing the effective mass by compression.* After the previous considerations, the next obvious idea is to reduce the effective mass by compression, to be achieved, e.g., by epitaxial stress or strain. Calculations for a 5% reduction of the lattice constant show that only the effective mass of the heavy holes is appreciably affected, while the light hole bands are not much altered. However, what is important for a small  $\kappa$  is the light-hole behavior; thus  $\kappa(E_F)$  does not change practically, and there is no increase in  $J_{nn'}$ . Actually for large distances we do obtain small changes in  $J_{nn'}$  after compression, but towards antiferromagnetic behavior. This has probably two origins:<sup>28</sup> at smaller lattice constants, the band width increases and the exchange splitting becomes smaller, so that (i) the spin-down impurity band merges more with the valence band setting on a Ruderman-Kittel-Kasuya-Yosida (RKKY) behavior, and (ii) the antiferromagnetic superexchange, which is sensitive to the exchange splitting, increases.

–*Alloying with Sulfur.* Next we considered shifting the N impurity states closer to the valence band by proper alloying of MgO with a third component. In this respect,  $\text{MgO}_{1-y}\text{S}_y$  seemed promising, because MgS also crystallizes in the rock-salt structure, with a larger lattice parameter (5.2 Å) and a smaller, indirect band gap (experimental: 4.5 eV ; we find 2.25 eV within the LDA). Calculations in  $\text{MgO}_{1-y}\text{S}_y$  (which were carried out by changing the lattice constant according to Vegard's law)

showed that the O valence states end up higher than the S valence states (see Fig. 2(b)). This result is counter-intuitive if one takes into account only the electronegativity of the elements. We interpret it by observing that the stronger localization of the O and N  $2p$  states is responsible for a stronger on-site Coulomb repulsion, so that filled  $2p$  levels end up higher in energy than the more extended S  $3p$  levels. As a consequence, the valence band edge in  $\text{MgO}_{1-y-x}\text{S}_y\text{N}_x$  is again Oxygen-dominated, but the position of the N impurity band is closer to the Oxygen valence band edge, and there is a stronger hybridization of the N with the O states compared to  $\text{MgO}_{1-x}\text{N}_x$ , as can be seen in Fig. 2(a,b). Because of this, the pair exchange constants are more extended in  $\text{MgO}_{1-y-x}\text{S}_y\text{N}_x$ . Calculations of  $\text{MgO}_{0.45}\text{S}_{0.5}\text{N}_{0.05}$  showed an enhancement of  $J(R)$  at large distances by up to 10-20% compared to  $\text{MgO}_{0.95}\text{N}_{0.05}$ . Thus the Curie temperature increases by a factor of the same order, remaining small.

*-Doping with holes.* In principle, the double-exchange mechanism for ferromagnetism is most effective when the impurity band of one spin is exactly half-filled, while for the opposite spin is completely full (or empty). Then the energy gain in the ferromagnetic state by band-broadening is maximized. In  $\text{MgO}_{1-x}\text{N}_x$  this is not the case, as the N spin-down band is filled by  $2/3$ . Therefore, doping with holes could help, as  $E_F$  will be shifted downward to the middle of the impurity band. Note that we are not trying to achieve the analogue of Zener's hole-mediated  $p$ - $d$  exchange, but rather an improvement of the double-exchange mechanism. (Similar engineering has been proposed in transition-metal-doped DMS.<sup>29</sup>) We investigate this effect in a Mg-poor compound i.e.,  $\text{Mg}_{1-y}\text{O}_{1-x}\text{N}_x$ . Each missing Mg atom adds two holes; thus the “ideal” Mg-vacancy concentration, resulting in exactly half-filling of the N spin-down band, is  $y = x/4$ . In our calculations we used  $x = 10\%$  and  $y = 2.5\%$ . As it turns out, the exchange interactions become more extended in space, however, the reason is that  $E_F$  now slightly enters the O valence band (since the valence band top is anyhow merged with the lower part of the impurity band), and a Fermi surface is now available for the impurity interaction. As a result, a RKKY mechanism emerges, with an outcome of also antiferromagnetic interactions at large distances. The latter turn out to be comparatively strong, once more because of an additional increase of superexchange, as  $E_F$  shifts closer to the spin-up band. Thus there is no increase of  $T_C$ . Tests with lower hole-doping concentration, before the RKKY exchange sets in, result in only a marginal increase of the long-range interactions, insufficient for a significant increase of  $T_C$ .

## V. DISCUSSION ON APPROXIMATIONS

### A. Approximations in the calculation of the electronic structure and Curie temperature

We now consider which approximations used in our calculations could most seriously affect the electronic structure, exchange constants and Curie temperature. Perhaps the most critical is the local density approximation. Corrections that could qualitatively change the electronic structure include self-interaction correction, inclusion of strong on-site Coulomb repulsion, or  $GW$ -type of self-energy.

In Ref. 10, Droghetti and Sanvito applied the self-interaction correction (SIC) to MgO doped with N (among other compounds). They find that an application of SIC to both N and O atoms increases the gap, as is expected by driving the occupied levels lower by the SIC. However, their main finding connected to our present discussion is the occurrence of a strong splitting of the order of 3 eV between the occupied and unoccupied  $p$  states of N. The spin-down impurity band is, after SIC, manifestly insulating. A similar effect was found within the LDA+ $U$  method, applied by Pardo and Pickett<sup>11</sup> to a number of oxides (including MgO) with N substitution of Oxygen. In the latter work, a Coulomb repulsion of  $U = 5.5$  eV was used on the O and N atoms. From the point of view of ferromagnetism, an insulating impurity band can have severe consequences, in particular disfavoring the double-exchange mechanism (impurity-band broadening does not lead to energy gain any more); ferromagnetic superexchange could be present, but it is much weaker. In these cases, the system could even show a spin-glass ground state instead of a ferromagnetic one.

These works demonstrate possible consequences of strong Coulomb interactions, showing that local density-functional theory could be insufficient. We believe that, at low concentrations, these results undoubtedly show the correct physics, but at higher concentrations (a few percent) they possibly overestimate the Coulomb interaction, and are therefore still inconclusive as to the exact nature of the ground state. Our arguments are as follows.

First, considering the low-concentration limit, the N impurity states are not localized at the N atomic cell, but rather extended also over the 12 nearest Oxygen neighbors, as our calculation shows. This speaks for a relatively mild self-interaction error, compared to  $d$ - or  $f$ -systems, where the SIC is usually applied to. The LDA error must become less and less serious as the concentration increases and an itinerant impurity band is formed. Furthermore, application of Coulomb correction terms on the Oxygen valence band is probably much less necessary, as the associated Bloch states are itinerant with a significant band width (in the limiting case of completely non-localized states of a homogeneous electron gas, the self-interaction is fully corrected by the LDA exchange-correlation energy). We conclude that Coulomb-interaction corrections should be of different

scale at the N impurity-band states compared to the O valence-band states, but even for N they should not be too severe.

Second, as the concentration  $x$  increases, the impurity band width  $w \sim \sqrt{x}$  increases rather fast, exceeding 1 eV already at  $x = 5\%$ . This band width can well be of the order of magnitude of the local Coulomb interaction  $U$  (in the LDA+ $U$  calculations of Ref. 11, a value of  $U = 5.5$  eV was used, which, however, acts on the atomic site; if the full extent of the impurity wavefunction is accounted for, a significantly lower value of  $U$  would be needed for the same effect). In this case a Mott transition is possible, from an insulating state for low concentrations (where  $w < U$ ) to a metallic state at high concentrations (where  $w > U$ ). In such a scenario, ferromagnetism would be assisted by the increase of concentration in two ways: occurrence of a metallic state similar to the LDA result, and magnetic percolation.

Concerning  $GW$ -type of corrections, these are known to correct the LDA underestimation of band gap in band insulators. It should be then expected that the larger gap would lead to a stronger decay of the exchange constants with distance, reducing the calculated  $T_C$ . However, this reduction should not be too serious, for the same reason that  $T_C$  cannot be much increased by engineering a smaller gap (see Sec. IV).

Another approximation that was made here was the assumption of a classical, rather than quantum, Heisenberg model to describe the magnetic excitations. Considering that we are faced with an  $S = \frac{1}{2}$  system, it can be argued that a classical approximation is unrealistic. Within the RPA, a change from a classical to a quantum Heisenberg model leads to an increase of  $T_C$  by a factor of  $S(S+1)/S^2 = 3$ , in the  $S = \frac{1}{2}$  case. Accepting this, room-temperature ferromagnetism could be achieved at  $x = 20\%$ , as can be seen by scaling up the results of Fig. 6. However, the particular way of calculation of the exchange coupling constants<sup>22</sup>  $J_{nn'}$  tacitly assumes a classical model. The constants are calculated within constrained density-functional theory, in principle by “freezing” the system in a static non-collinear configuration and calculating the total energy; this should be viewed as a parametrization of the low-energy excitations of the spin density, rather than a derivation of a quantum spin Hamiltonian. Comparison to experiments in previous works also advocates for this point of view. E.g., Sasioglu et al.<sup>30</sup> have calculated the Curie temperature of Heusler alloys by a similar recipe. While the assumption of a classical Heisenberg model lead them to reasonable agreement of  $T_C$  with experiment, the assumption of a quantum model resulted in a clear overestimation of  $T_C$ . For lack of a better theory that predicts  $J_{nn'}$  for a quantum Heisenberg model, we are obliged to work within a classical model.

## B. Approximations imposed by our structural model

So far we assumed a uniform, on the average, distribution of the N atoms in the MgO matrix. We therefore start this Subsection by commenting on the solubility of N in MgO. The solubility limit of substitutional N is expected to be small, and clustering of the N impurities is expected to be favored. We verified this by calculating, within the KKR-CPA, the mixing energy as a function of the concentration,  $E_{\text{mix}}(x) = E[\text{MgO}_{1-x}\text{N}_x] - (1-x)E[\text{MgO}] - xE[\text{MgN}]$  with MgN in the rock-salt structure.  $E_{\text{mix}}(x)$  was positive for all calculated concentrations ( $1\% \leq x \leq 90\%$ ), showing that phase separation into MgO and MgN is energetically favored. This can be understood also from the local density of states, shown in Fig. 2(a), where it is seen that the impurity band is bisected by the Fermi level  $E_F$ . In case of impurity clustering the bandwidth will increase and energy will be gained because of the lowering of the occupied levels. Interestingly, the origin of ferromagnetic double exchange (bisection of the impurity band by  $E_F$ ) provides also a mechanism for (usually unwanted) phase separation. Of course, phase separation other than the MgO-MgN type could be also possible; what this calculation shows is the thermodynamic instability of  $\text{MgO}_{1-x}\text{N}_x$  with respect to at least one type of phase separation, even if entropic effects could milder the separation. The preference toward clustering was also seen in calculations of two substitutional N impurities in a MgO supercell matrix: the most stable state was found when the two N atoms were first neighbors in the  $\langle 110 \rangle$  direction. We conclude that  $\text{MgO}_{1-x}\text{N}_x$  can only be grown under out-of-equilibrium conditions, as is the case with many transition-metal-doped DMS.

Two neighboring substitutional N atoms still provide a metallic state. However, three neighboring N atoms forming an equilateral triangle in a  $\{111\}$  plane cause a transition to a semiconducting state (with a split minority-spin band), if structural optimization of the three atoms and their surroundings is taken into account.

Coming now to interstitial N impurities, our calculations (performed with VASP) showed that strong atom displacements are involved, thus we cannot use CPA to describe the random alloy with interstitials. As the phase space involved is extremely rich, and probably depends strongly on growth and annealing conditions, we defer a deeper analysis of the particular question to a future work, commenting on a few interesting findings.

First, in the case of a single N interstitial, the symmetric, tetrahedral position constitutes only a local minimum of the total energy. Further significant reduction of the total energy is found in a “dumbbell” configuration reminiscent of a NO molecule, where the N impurity binds itself to an O atom, with both atoms in the proximity of the ideal O lattice position. This entity is found to be half-metallic and magnetic, with a moment of  $1 \mu_B$ .

Second, when two Nitrogen atoms are placed around

an Oxygen atom as interstitials, structural relaxation leads to a “zig-zag” O-N-O-N configuration. Here, the two N atoms are almost on the lattice sites, being first neighbors along  $\langle 110 \rangle$ , while the O atoms are shifted out of their ideal positions, hovering above the  $\langle 110 \rangle$  atomic layer. The electronic structure changes to non magnetic and insulating.

Third, the following configuration is of particular interest: two neighboring N atoms together with an O interstitial between them, plus a nearby O vacancy. This is so to say a configuration where an O atom has been bound during growth by a N pair, missing the lattice position nearby. This configuration shows a local energy minimum and is non-magnetic. However, if the O atom returns to the vacant lattice position, the state becomes magnetic with a total energy gain of the order of 4 eV, while the lattice parameter is reduced by 1% (in the particular calculation we took a  $\text{Mg}_{32}\text{O}_{30}\text{N}_2$  supercell, corresponding to 6.25% N). This is a possible explanation of the appearance of magnetism after annealing in experiment.<sup>18</sup>

## VI. CONCLUSIONS AND OUTLOOK

The chemical compound  $\text{MgO}_{1-x}\text{N}_x$  in which Oxygen is substituted by Nitrogen atoms is found to be ferromagnetic for all concentrations which seem realistically achievable ( $x \leq 15\%$ ) and above the concentration of the percolation threshold (about 1.5%). The N atom forms a partially occupied gap state at the vicinity of the valence band edge. This leads to concentration-dependent exchange parameters, exponentially decreasing with distance, which are ferromagnetic due to double exchange as dominating mechanism. The reduction of the average N-N distance and the reduction of the exchange interaction strength with increasing concentration compensate partially, so that the Curie temperature increases linearly with concentration. The structural relaxation around the N impurity are found to be small. In the case of N clusters and interstitial N we found magnetic as well as non-magnetic complexes, but never with higher moments than  $1 \mu_B/\text{atom}$ .

We think that the Curie temperature of such *sp*-compounds can be increased if the exchange interactions become more long-ranged, e.g. by moving the gap states closer to the band edge, and if the N-N exchange interactions are enhanced by suppressing the competing antiferromagnetic superexchange via an increase of the local exchange splitting. Our attempts in this direction, using compounds such as  $\text{MgO}_{1-x-y}\text{S}_y\text{N}_x$  or  $\text{Mg}_{1-y}\text{O}_{1-x}\text{N}_x$ , have not been met with success. Nevertheless, it is worthwhile to investigate more host/impurity combinations theoretically, in order to guide experimental efforts.

From the point of view of applications, a low  $T_C$  is a limiting factor. However, from the point of view of physics, *sp* magnetism in oxides presents intriguing open problems, such as the nature of the ground state, its con-

centration dependence, and the role of dynamic electron correlations. Moreover, although homogeneous Nitrogen distributions at high concentrations are difficult to achieve, it is worthwhile to examine the physics and technological relevance of inhomogeneous samples, emerging, e.g., by spinodal decomposition<sup>32</sup> or delta-doping,<sup>26</sup> as has been proposed for transition-metal doped DMS. Such compounds could show much more robust magnetism locally, leading to new functionalities.

## APPENDIX A: METHODS OF CALCULATION

For the calculations of the alloy ground-state electronic structure (except structural relaxations) we used the full-potential Korringa-Kohn-Rostoker Green-function method<sup>31</sup> (KKR) with exact calculation of the atomic cell shapes,<sup>33</sup> using an angular momentum cutoff of  $l_{\text{max}} = 3$  and a maximal  $k$ -point mesh of 64000 points in the full Brillouin zone; the complex-energy contour integration included the Oxygen and Nitrogen  $2s$  states. Disorder was treated within the Coherent Potential Approximation (KKR-CPA). Relativistic effects were neglected. In the KKR-CPA calculations we used the MgO experimental lattice parameter for all concentrations, as the small change should have no significant effect in the calculated trends.

For the calculation of the hole localization, the impurity-in-host version of the KKR method was employed non-self-consistently, with potentials taken from self-consistent CPA. In the KKR-CPA calculations, the LDA for the exchange-correlation energy was used with the parametrization of Vosko et al.<sup>34</sup> For the structural relaxations we used the Vienna *ab-initio* simulation package<sup>19</sup> (VASP) within the GGA.<sup>35</sup>

The exchange constants  $J_{nn'}$  were calculated within the approximation of infinitesimal rotations,<sup>22</sup> again within the KKR-CPA. As has been found by Sato et al.,<sup>36</sup> the method of infinitesimal rotations within the CPA can overestimate the values of  $J_{nn'}$  between the nearest neighbors at low concentrations (when they anyhow are irrelevant for  $T_C$ ), but is rather good for larger distances.

The Curie temperatures were calculated within the random-phase approximation (RPA) for disordered systems, as proposed by Hilbert and Nolting,<sup>17</sup> with the distance-dependent interactions  $J_{nn'}$  taken as described above. At each concentration, an environmental average was evaluated by taking 100 random configurations of approx. 8500 nitrogen atoms each, statistically distributed in a simulation supercell (sized between  $21^3$  unit cells for 90% concentration and  $94^3$  unit cells for 1% concentration). To each configuration the RPA yielded a  $T_C$ , and an average of all values of  $T_C$  was determined at the end. In special cases ( $x = 5\%$ ,  $10\%$ ,  $15\%$  and  $10\%$ ) the results were cross-checked with Monte Carlo calculations, which yielded a  $T_C$  of approximately 50% higher, except for 5% where the results of the two methods agreed. Because



the Monte Carlo method is numerically more expensive, in these tests we treated systems of 1000-2500 magnetic ions, using up to 20 configurations for averaging; within Monte-Carlo,  $T_C$  was calculated using the 4th order cumulant method.<sup>37</sup>

## ACKNOWLEDGMENTS

We would like to thank Stuart Parkin for discussions on his experimental results prior to publication. We

are grateful to Peter H. Dederichs for his constant support and enlightening discussions. This work was funded in part by the Young Investigators Group Programme of the Helmholtz Association ("Computational Nanofotonics Laboratory," Contract VH-NG-409).

- 
- \* Electronic address: Ph.Mavropoulos@fz-juelich.de  
† Electronic address: M.Lezaic@fz-juelich.de
- <sup>1</sup> F. Máca, J. Kudrnovský, V. Drchal, and G. Bouzerar, Appl. Phys. Lett. **92**, 212503 (2008); F. Máca, J. Kudrnovský, V. Drchal, and G. Bouzerar, Philos. Mag. **88**, 2755 (2008).
  - <sup>2</sup> C.D. Pemmaraju and S. Sanvito, Phys. Rev. Lett. **94**, 217205 (2005).
  - <sup>3</sup> J. Osorio-Guillén, S. Lany, S. V. Barabash, and A. Zunger, Phys. Rev. Lett. **96**, 107203 (2006); J. Osorio-Guillén, S. Lany, S. V. Barabash, and A. Zunger, Phys. Rev. B **75**, 184421 (2007).
  - <sup>4</sup> G. Bouzerar and T. Ziman, Phys. Rev. Lett. **96**, 207602 (2006).
  - <sup>5</sup> K. Kenmochi, M. Seike, K. Sato, A. Yanase, and H. Katayama-Yoshida, Jpn. J. Appl. Phys. **43**, L934 (2004).
  - <sup>6</sup> K. Kenmochi, V. A. Dinh, K. Sato, A. Yanase, and H. Katayama-Yoshida, J. Phys. Soc. Jpn **73**, 2952 (2004).
  - <sup>7</sup> Van An Dinh, K. Sato, and H. Katayama-Yoshida, Solid State Commun. **136**, 1 (2005).
  - <sup>8</sup> I.S. Elfimov, A. Rusydi, S. I. Csiszar, Z. Hu, H. H. Hsieh, H.-J. Lin, C. T. Chen, R. Liang, and G. A. Sawatzky, Phys. Rev. Lett. **98**, 137202 (2007).
  - <sup>9</sup> V.V. Bannikov, I.R. Shein, and L. Ivanovskii, Techn. Phys. Lett. **33**, 541 (2007).
  - <sup>10</sup> A. Droghetti, C.D. Pemmaraju, and S. Sanvito, Phys. Rev. B **78**, 140404(R) (2008).
  - <sup>11</sup> V. Pardo and W. E. Pickett, Phys. Rev. B **78**, 134427 (2008).
  - <sup>12</sup> Bo Gu, Nejat Bulut, Timothy Ziman, and Sadamichi Maekawa, Phys. Rev. B **79**, 024407 (2009).
  - <sup>13</sup> A. Droghetti and S. Sanvito Appl. Phys. Lett. **94**, 252505 (2009).
  - <sup>14</sup> M. Sieberer, J. Redinger, S. Khmelevskiy, and P. Mohn, Phys. Rev. B **73**, 024404 (2006).
  - <sup>15</sup> K. Sato, W. Schweika, P.H. Dederichs, and H. Katayama-Yoshida, Phys. Rev. B **70**, 201202(R) (2004).
  - <sup>16</sup> L. Bergqvist, O. Eriksson, J. Kudrnovsky, V. Drchal, P. Korzhavyi, and I. Turek, Phys. Rev. Lett. **93**, 137202 (2004).
  - <sup>17</sup> S. Hilbert and W. Nolting Phys. Rev. B **70**, 165203 (2004).
  - <sup>18</sup> S.S.P. Parkin, private communication. See also C.-H. Yang, M. Samant, and S. Parkin, 2009 APS March Meeting Abstract V22.00004, <http://meetings.aps.org/Meeting/MAR09/Event/98745>
  - <sup>19</sup> The Vienna *ab-initio* simulation package, G. Kresse and J. Hafner, Phys. Rev. B **47**, R558 (1993); G. Kresse, Thesis, Technische Universität Wien (1993); G. Kresse and J. Furthmüller, Comput. Mat. Sci. **6**, 15 (1996); G. Kresse and J. Furthmüller, Phys. Rev. B **54**, 11169 (1996); G. Kresse, and J. Joubert, Phys. Rev. B **59**, 1758 (1999); P.E. Blchl, Phys. Rev. B **50**, 17953 (1994).
  - <sup>20</sup> H. Akai, Phys. Rev. Lett. **81**, 3002 (1998).
  - <sup>21</sup> L.M. Sandratskii and P. Bruno, Phys. Rev. B **73**, 045203 (2006).
  - <sup>22</sup> A.I. Liechtenstein, M.I. Katsnelson, V.P. Antropov, and V.A. Gubanov, J. Magn. Magn. Mater. **67** 65 (1987).
  - <sup>23</sup> B. Belhadji, L. Bergqvist, R. Zeller, P.H. Dederichs, K. Sato, and H. Katayama-Yoshida, J. Phys.: Condens. Matter **19**, 436227 (2007).
  - <sup>24</sup> M. Pajda, J. Kudrnovský, I. Turek, V. Drchal, and P. Bruno, Phys. Rev. B **64**, 174402 (2001).
  - <sup>25</sup> L.M. Sandratskii and P. Bruno, Phys. Rev. B **67**, 214402 (2003); J. Kudrnovský, V. Drchal, I. Turek, L. Bergqvist, O. Eriksson, G. Bouzerar, L. Sandratskii, and P. Bruno, J. Phys.: Condens. Matter **16** S5571 (2004); S. Picozzi and M. Lezaic, New J. Phys. **10**, 055017 (2008).
  - <sup>26</sup> S. Picozzi, M. Lezaic, and S. Blügel, Phys. Status Solidi A **203**, 2738 (2006).
  - <sup>27</sup> P.H. Dederichs, P. Mavropoulos, O. Wunnicke, N. Papanikolaou, V. Bellini, R. Zeller, V. Drchal, and J. Kudrnovský, J. Magn. Magn. Mater. **240** 108 (2002); P. Mavropoulos, N. Papanikolaou, and P.H. Dederichs, Phys. Rev. Lett. **85**, 1088 (2000).
  - <sup>28</sup> L. Bergqvist, B. Belhadji, S. Picozzi, and P. H. Dederichs, Phys. Rev. B **77**, 014418 (2008).
  - <sup>29</sup> T. Fukushima, K. Sato, H.K. Yoshida, and P.H. Dederichs, Physica B: Condensed Matter **376-377**, 786 (2006).
  - <sup>30</sup> E. Sasioglu, L. M. Sandratskii, P. Bruno, and I. Galanakis, Phys. Rev. B **72**, 184415 (2005).
  - <sup>31</sup> The SPR-TB-KKR package, H. Ebert and R. Zeller, <http://olymp.cup.uni-muenchen.de/ak/ebert/SPR-TB-KKR>
  - <sup>32</sup> K. Sato, T. Fukushima and H. Katayama-Yoshida, J. Phys.: Condens. Matter **19** 365212 (2007).
  - <sup>33</sup> N. Stefanou and R. Zeller, J. Phys.: Condens. Matter **3**, 7599 (1991).
  - <sup>34</sup> S.H. Vosko, L. Wilk, and M. Nusair, Can. J. Phys. **58**, 1200 (1980).
  - <sup>35</sup> J. Perdew, K. Burke, and M. Ernzerhof, Phys. Rev. Lett. **77**, 3865 (1996).
  - <sup>36</sup> K. Sato, P.H. Dederichs, and H. Katayama-Yoshida, Phys. Stat. Sol. (c) **3**, 4143 (2006).
  - <sup>37</sup> D.P. Landau and K. Binder *A Guide to Monte Carlo Simulations in Statistical Physics*, Cambridge University Press,

Cambridge 2000.